

## Improved Structural Data of Cellulose III<sub>I</sub> Prepared in Supercritical Ammonia

M. Wada,<sup>†</sup> L. Heux,<sup>‡</sup> A. Isogai,<sup>†</sup> Y. Nishiyama,<sup>†</sup> H. Chanzy,<sup>‡</sup> and J. Sugiyama<sup>\*,§</sup>

Graduate School of Agricultural and Life Sciences, The University of Tokyo, Bunkyo-ku, Tokyo 113-8657, Japan; Centre de Recherches sur les Macromolécules Végétales (Affiliated with Joseph Fourier University of Grenoble), C.N.R.S. B.P. 53, 38401, Grenoble Cedex 9, France; and Wood Research Institute, Kyoto University, Kyoto 611-0011, Japan

Received August 9, 2000; Revised Manuscript Received December 7, 2000

**ABSTRACT:** Highly crystalline cellulose III<sub>I</sub> samples were prepared by subjecting oriented films consisting of an assembly of *Cladophora* cellulose microcrystals to supercritical ammonia. Diffraction data recorded on these specimens indicated that the crystals of cellulose III<sub>I</sub> could be fully described with a one-chain unit cell and a  $P2_1$  space group, with the cellulose chain axis on one of the  $2_1$  screw axes of the cells. The new cell had the following parameters:  $a = 0.448$  nm,  $b = 0.785$  nm,  $c$  (chain axis) = 1.031 nm,  $\gamma = 105.1^\circ$ . In this cell, which is half of the one proposed so far for cellulose III<sub>I</sub>, one glucosyl residue becomes the asymmetric unit. A good agreement between the diffraction analysis and spectroscopic data was observed.  $^{13}\text{C}$  CP/MAS spectra of the samples presented only six sharp resonance peaks, attributed to the six carbons of the asymmetric glucosyl residue. In these spectra, the occurrence of the C6 signal at 62.3 ppm is a clear indication that the hydroxymethyl moiety is in the *gt* conformation. FT-IR spectra of cellulose III<sub>I</sub> were recorded that showed that in the OH stretching region, there was only one very sharp absorption band that was polarized parallel to the fiber direction as opposed to two broad bands polarized perpendicular. A comparison of the spectroscopic data of cellulose III<sub>I</sub> with those of the other cellulose allomorphs suggest that the single chain of cellulose III<sub>I</sub> may have some conformational similarities with one of the two chains existing in the crystal of cellulose II.

### Introduction

The development of high-resolution  $^{13}\text{C}$  cross-polarization/magic-angle spinning nuclear magnetic resonance (CP/MAS NMR) techniques during the past two decades have brought new dimensions to the structural study of cellulose, ranging from its crystal structure to its polymorphism. It is due to this emerging technique that it became clearly established in 1984 that native celluloses (or cellulose I) from the cell wall of some marine green algae consisted of two distinct crystalline allomorphs, namely, cellulose I $_{\alpha}$  and I $_{\beta}$ .<sup>1</sup> By extension of such spectroscopic analyses to other specimens, it was revealed that all native cellulose samples contained the two allomorphs but in various proportion depending on the sample origin.<sup>2–5</sup> This important discovery has prompted a number of studies dedicated to the reinvestigation of the crystalline structure of cellulose I established before the input of the  $^{13}\text{C}$  CP/MAS NMR solid-state data.<sup>6,7</sup> So far, only the unit cells of cellulose I $_{\alpha}$  and I $_{\beta}$  has been experimentally measured as a result of electron diffraction analysis.<sup>8</sup> Despite this progress, the exact atomic coordinates and hydrogen bonding system of cellulose I $_{\alpha}$  and I $_{\beta}$  remain to be determined. A number of modeling studies have aimed to describe cellulose I $_{\alpha}$  and I $_{\beta}$ ,<sup>9–11</sup> but so far, none of these has been verified by X-ray analysis.

Cellulose II or recrystallized cellulose is a third cellulose allomorph for which  $^{13}\text{C}$  CP/MAS NMR data have played a key role in the structure refinement. Before the advent of this spectroscopy, the structure of cellulose II, refined in 1976, was believed to consist of

a two-chain  $P2_1$  unit cell where the two chains were crystallographically independent and of opposite polarity.<sup>12,13</sup> The two chains were thought to have conformations that were identical for their backbones, but different for their hydroxymethyl groups. The conformation of these moieties was believed to be near *gt* for the chain located at the origin and *tg* for the center chain.<sup>14</sup> The hypothesis of these two conformations has now been challenged by  $^{13}\text{C}$  CP/MAS NMR data, which indicate that the C6 resonance of the hydroxymethyl group occurs as a singlet near 64 ppm in cellulose II.<sup>15,16</sup> If both *gt* and *tg* conformations had been present, a doublet with significantly separated resonances near 64 and 66 ppm should have occurred.<sup>17</sup> In light of this contradiction and following X-ray crystallography analyses on cellodextrin models,<sup>18–20</sup> the structure of cellulose II has been revised using the 1976 data sets.<sup>21,22</sup> In this revised structure, the two independent hydroxymethyl groups are in *gt* and the two chains have different conformations. There is therefore a good agreement between the hydroxymethyl conformation deduced from the X-ray and those of  $^{13}\text{C}$  CP/MAS NMR data. The revised structure of cellulose II has been recently confirmed by a diffraction analysis resulting from neutron data sets.<sup>23</sup>

Cellulose III<sub>I</sub> is another cellulose allomorph that results from the treatment of cellulose I by liquid ammonia or by series of amines.<sup>24,25</sup> The  $^{13}\text{C}$  CP/MAS spectrum of cellulose III<sub>I</sub> is unique in the series of cellulose allomorphs since in cellulose III<sub>I</sub> each carbon atom shows only a single resonance,<sup>16,26</sup> in contrast with the spectra of other allomorphs where most of the carbon atoms display multiple resonances. For cellulose, this behavior is a strong indication that the asymmetric unit of the crystal of cellulose III<sub>I</sub> is in fact one glucosyl residue. This deduction is in contradiction with the

\* Fax: 81-774-38-3635. E-mail: junjis@kuwri.kyoto-u.ac.jp.

<sup>†</sup> The University of Tokyo.

<sup>‡</sup> Centre de Recherches sur les Macromolécules Végétales.

<sup>§</sup> Kyoto University.

proposed structure of cellulose III<sub>I</sub>, which indicates that this allomorph is crystallized in a  $P2_1$  space group with two independent cellulose chains per unit cell, located on the  $2_1$  screw axes of the structure.<sup>27</sup> If this structure were correct, there should be two independent glucosyl moieties in the crystal, and this situation should induce some splitting in the carbon signals of the <sup>13</sup>C CP/MAS spectra. As such splitting is not seen, it is likely that the X-ray structure of cellulose III<sub>I</sub> needs to be revised.

The present work deals with our attempts to prepare adequate samples of cellulose III<sub>I</sub> susceptible to yield improved crystallographic and spectroscopic data. Advantage was taken from a recent method devised to prepare highly crystalline samples of cellulose III<sub>I</sub> by using a supercritical ammonia treatment.<sup>28,29</sup> This paper reports preliminary structural data resulting from the analysis of such samples, using conventional X-ray, synchrotron and electron diffraction, FT-IR, and <sup>13</sup>C NMR spectroscopies.

## Experimental Section

**Cellulose Samples.** *Cladophora*, a green alga, was harvested in Chikura, Chiba Pref., Japan, and was purified by a repetitive treatment with 5% KOH and 0.3% NaClO<sub>2</sub> solutions. The purified sample, which was homogenized into small fragments, was treated with 50% sulfuric acid at 70 °C for 8 h under continuous stirring. This treatment converted the initial cellulose crystals into a suspension of cellulose microcrystals. The suspensions were then washed with deionized water by successive dilution and centrifugation until the supernatant became turbid. These suspensions were dialyzed against deionized water for a few days, dispersed with a sonicator probe for 1 min and finally treated with mixed-bed ion-exchange resin.

Thin films of cellulose microcrystals with random orientation were obtained by casting the suspension on glass plates followed by drying in air for a few days. The films were further dehydrated at 50 °C for 24 h and stored in a desiccator until usage.

Oriented films of cellulose microcrystals were prepared according to the method of Nishiyama et al.<sup>30</sup> These films were dried at 105 °C for 8 h and stored in a desiccator until usage.

Specimens of tunicate cellulose and *Glaucocestis* chosen respectively as standards for cellulose I<sub>β</sub> and I<sub>α</sub> were prepared as described elsewhere.<sup>31,32</sup> Microcrystalline rayon was chosen as a standard for cellulose II. This sample was prepared according to the method of Battista.<sup>33</sup>

**Conversion into Cellulose III<sub>I</sub>.** The oriented cellulose films were inserted into a steel pressure vessel, which was cooled in a dry ice/methanol bath. Ammonia was liquefied into the vessel until the samples were totally immersed. The vessel was then sealed and brought to room temperature. This temperature was kept for 30 min, followed by heating in an oil bath to 140 °C, a temperature higher than 132.5 °C which is the critical temperature of ammonia. This temperature was maintained for 1 h, the vessel was removed from the oil bath, and the ammonia gas was immediately leaked out as gas, under strong ventilation. The treated samples were then thoroughly washed with dry methanol and dried under high vacuum at 50 °C.

**X-ray and Synchrotron Diffraction Experiments.** Fiber diffraction diagrams of the oriented cellulose III<sub>I</sub> films were obtained with a flat-plate vacuum camera mounted on a Rigaku RU-200BH rotating anode X-ray generator, operated at 50 kV and 100 mA. The diagrams were recorded with Ni-filtered Cu K<sub>α</sub> radiation ( $\lambda = 0.15418$  nm), collimated with a pinhole of  $\phi$  0.3 mm. X-ray diffraction patterns were recorded on Fuji imaging plates (IP), and the IP-to-sample distance was calibrated using NaF ( $d = 0.23166$  nm). A unit cell was refined from the indexation and calibration of the diffraction spots and a reliability parameter  $R_{\text{X-ray}}$  was calculated as follows,  $R_{\text{X-ray}} = [\sum(d_o - d_{\text{cal}})^2 / \sum d_o^2]^{1/2}$ , where the  $d_o$ 's correspond to the

observed  $d$ -spacings and the  $d_{\text{cal}}$ 's correspond to the calculated  $d$ -spacings.

The oriented cellulose III<sub>I</sub> films were also analyzed at the ID2 beamline at the European Synchrotron Radiation Facility (ESRF), Grenoble, France. The samples, which were positioned at the center of a Huber five-circle goniometer, were irradiated for 20 s with synchrotron radiation ( $\lambda = 0.0720006$  nm). The diffraction patterns were recorded on a MAR imaging plate positioned at 170 mm from the sample. The patterns were analyzed with the *LSQUINT* program from the *CCP13* software package. The unit cell was refined from the calibration and indexation of the diffraction spots and a reliability factor  $R_{\text{sync}}$  was calculated as follows  $R_{\text{sync}} = [\sum(P_o - P_{\text{cal}})^2 / \sum P_o^2]^{1/2}$ , where the  $P_o$ 's are the observed pixels coordinates of the diffraction spots and the  $P_{\text{cal}}$ 's are the corresponding calculated pixel values.

**Electron Microscopy.** A 10  $\mu$ L aliquot of the microcrystalline suspension of cellulose III<sub>I</sub> was mounted on a carbon-coated hydrophilic grid. After being air dried, the grid was analyzed with a JEOL electron microscope (JEM 2000-EXII) operated at 100 kV and equipped with a GATAN image intensifier (model 622-0300). The electron micrographs of unstained specimens were taken under bright-field contrast diffraction mode, using low-dose exposure at 10 000 $\times$ . Electron microdiffraction experiments were performed both at room and low temperature, using a low-dose electron probe of approximately 0.1  $\mu$ m diameter area of the specimen. Low-temperature experiments were achieved to reduce radiation damage. For this, we used a GATAN cold stage (model 626) operated at liquid-nitrogen temperature. All of the images and microdiffraction were recorded on Mitsubishi MEM film.

**Solid-State <sup>13</sup>C MAS NMR Measurements.** NMR experiments were performed with a Bruker MSL spectrometer operated at a <sup>13</sup>C frequency of 25 MHz, using the combined techniques of proton dipolar decoupling (DD), magic-angle spinning, and cross-polarization. <sup>13</sup>C and <sup>1</sup>H field strengths of 64 kHz corresponding to 90° pulses of 4  $\mu$ s were used for the matched spin-lock cross-polarization transfer. The spinning speed was set at 3000 Hz. The contact time was 1 ms, the acquisition time 70 ms, the sweep width 29 400 Hz, and the recycling delay 4 s. A typical number of 10 000 scans were acquired for each spectrum. Chemical shifts were referred to tetramethylsilane after calibration with the carbonyl signal of glycine at 176.03 ppm.

Cellulose III<sub>I</sub> is renown to hold inclusion solvents.<sup>34</sup> Since our samples have been washed and stored in dry methanol, the absence of such molecules as inclusion in our vacuum-dried samples was checked by single-pulse (SP/MAS) experiments. This technique did not reveal any additional signal for the vacuum-treated samples used in this study. On the other hand, if the vacuum-dried sample was soaked in methanol for 24 h, a sharp signal at 49.07 ppm was observed.

**FT-IR Measurement.** Thin cellulose III<sub>I</sub> films with random orientation were subjected to FT-IR measurements using a Nicolet Magna 860 spectrometer operated under nonpolarized radiation. All spectra were recorded with an accumulation of 64 scans and a resolution of 4 cm<sup>-1</sup> in the range from 4000 to 400 cm<sup>-1</sup>. Polarized FT-IR spectra were obtained with a Perkin-Elmer 1720X spectrometer fitted with a gold wire grid polarizer. With polarized infrared, when a band is greater with perpendicular radiation, this band is denoted ( $\perp$ ). When the reverse is true, the band is denoted as parallel ( $\parallel$ ) band.

## Results

**X-ray Diffraction Data.** Two X-ray fiber diffraction diagrams of cellulose III<sub>I</sub>, resulting from conventional X-ray and synchrotron experiments, are shown in parts a and b of Figure 1, respectively. Both diagrams display a fairly high resolution: better than 0.2 nm in Figure 1a and better than 0.1 nm in Figure 1b. In both diagrams, one can remark the presence of a very strong 002 reflection. Such reflection, which is weak in celluloses I and II, can be considered a signature for cellulose



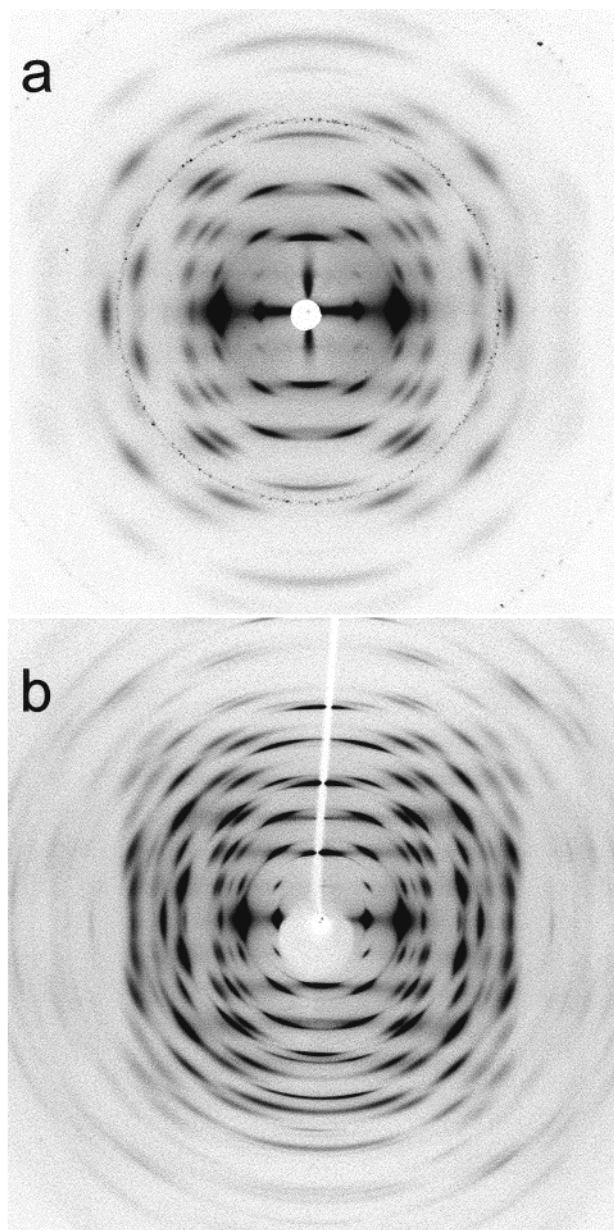


**Figure 1.** X-ray fiber diffraction diagrams of vertically oriented films of cellulose III<sub>I</sub> from *Cladophora* recorded with conventional X-ray with (a) Cu K $\alpha$  and (b) synchrotron radiation.

III<sub>I</sub>. In both diagrams, the absence of equatorial reflections at 0.6 and 0.54 nm or at 0.43 on the second layer line is a clear indication that there is no leftover cellulose I in these samples.

The analysis of the X-ray fiber diagram in Figure 1a yields 30 independent reflections within five layer-lines. All of these reflections can be indexed according to a one-chain monoclinic unit cell with dimensions  $a = 0.443$  nm,  $b = 0.785$  nm,  $c$  (chain and unique axis) = 1.031 nm, and  $\gamma = 104.7^\circ$ , with a reliability parameter  $R_{x\text{-ray}} = 0.4\%$ . On the meridian of this diagram, and in addition to the very strong 002, one denotes the following: 001, absent, 003, weak, 004, medium, and 005 absent. With the exception of the weak 003, the presence and absence of these reflections are consistent with those corresponding to space group  $P2_1$ , with the  $2_1$  axis along the fiber axis. The synchrotron fiber diffraction shown in Figure 1b can also be indexed in the same  $P2_1$  space group. Its resolution goes beyond

**Table 1. Chemical Shifts for the C1, C4, and C6 of Some of the Cellulose Allomorphs**

	chemical shifts (ppm)		
	C1	C4	C6
cellulose I $_{\alpha}$ ( <i>Glaucocystis</i> )	105.0	89.7, 88.8	65.3
cellulose I $_{\beta}$ (tunicin)	105.7, 103.9	88.7 88.0	65.5, 64.9
cellulose II (microcrystalline rayon)	107.0, 104.7	88.4, 87.3	62.9, 62.2
cellulose III <sub>I</sub> (prepared in supercritical ammonia)	104.8	87.8	62.3

0.1 nm. It displays 114 individual reflections within nine layer lines. Again, this diagram is also consistent with a  $P2_1$  space group and a one-chain unit cell with dimensions of  $a = 0.448$  nm,  $b = 0.785$  nm,  $c$  (chain axis) = 1.031 nm, and  $\gamma = 105.13^\circ$ , with a reliability factor  $R_{\text{sync}} = 0.39\%$ .

**Electron Microscopy and Electron Diffraction Data.** A typical sample of cellulose III<sub>I</sub> is presented in Figure 2. This sample consists of series of whiskerlike crystals with sharp contours, similar to the parent cellulose I crystals.<sup>35</sup> Thus by converting crystals of cellulose I into cellulose III<sub>I</sub>, there is no visible effect on the morphology of the individual crystals. When probed by electron microdiffraction, each crystal of cellulose III<sub>I</sub> gave a sharp spot diagram, indicating that each of these elements is indeed a single crystal. Thus, there is a solid-state conversion where apparently one cellulose I crystal yields one cellulose III<sub>I</sub> crystal. When the electron diffraction patterns were recorded at either room or liquid-nitrogen temperature, most of the diffraction spots corresponded to pure cellulose III<sub>I</sub> and could be indexed along the one-chain unit cells defined in the above section. A pattern such as the one shown as an inset in Figure 2 is consistent with a monoclinic space groups. In addition, since only 002, 004, and 006 are present along the  $c^*$  axis, the assignment of  $P2_1$  that could have been questioned from the X-ray and synchrotron diffraction data appears justified. In some of the patterns recorded at room temperature, four extra weak spots with  $d$ -spacings of 0.434 nm on the second layer line were also observed. These extra spots were identified as corresponding to the reflection 102 and its three mirrors from cellulose I. When the electron diffraction experiments were achieved at liquid-nitrogen temperature (inset in Figure 2), these extra spots were not observed.

**Solid-State  $^{13}\text{C}$  CP/MAS NMR Measurements.** The solid-state spectrum of cellulose III<sub>I</sub>, prepared in supercritical ammonia, is presented in Figure 3a. In Figure 3, we also show for comparison the spectra of other cellulose allomorphs recorded under similar conditions: celluloses II (Figure 3b), I $_{\beta}$  (Figure 3c), and I $_{\alpha}$  (Figure 3d). The dominant feature of the spectrum of cellulose III<sub>I</sub> is that it presents only six sharp peaks, obviously corresponding to the six carbon atoms of the glucosyl residue constituting cellulose. The chemical shifts of the peaks corresponding to C1, C4, and C6, together with those of the other allomorphs are listed in Table 1. A comparison of these values indicates that cellulose III<sub>I</sub> appears to have some features of cellulose II. A comparison of the chemical shifts of the peaks corresponding to C1, C4, and C6 to those of the other allomorphs indicates that cellulose III<sub>I</sub> appears to have some features of cellulose II. Indeed, the chemical shifts of C1 and C6 of cellulose III<sub>I</sub> are within experimental error exactly the same as the high field peaks of the C1 and C6 doublets of cellulose II. The chemical shift of

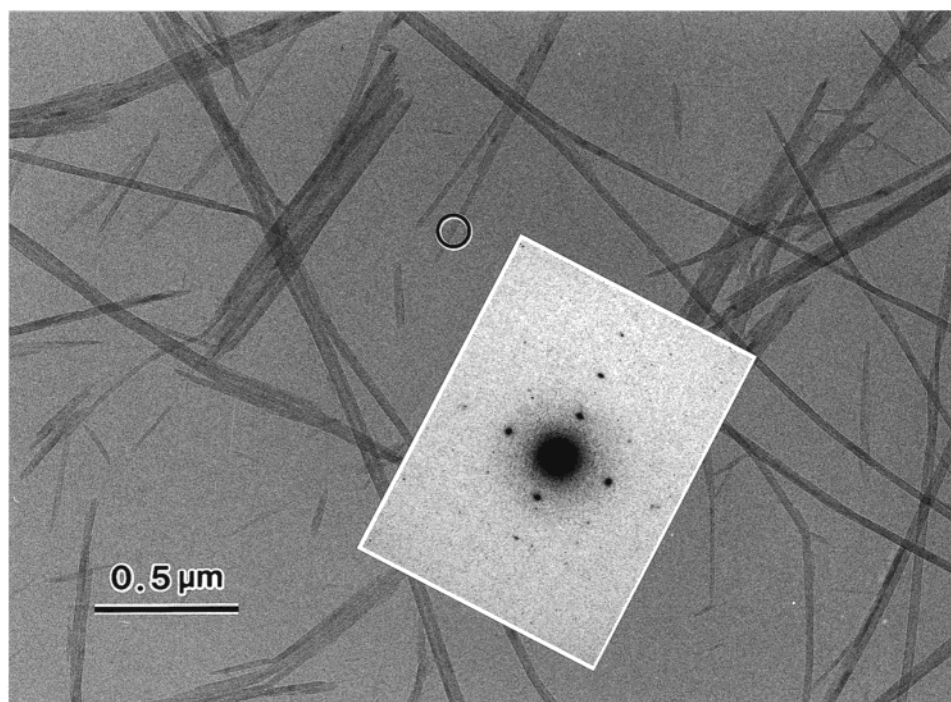


**Figure 2.** Transmission electron micrograph in low-dose bright-field of a diffraction-contrast image of a preparation of microcrystals of *Cladophora* cellulose converted into cellulose III<sub>I</sub>. Inset: typical microdiffraction pattern recorded on an area such as the circled one.

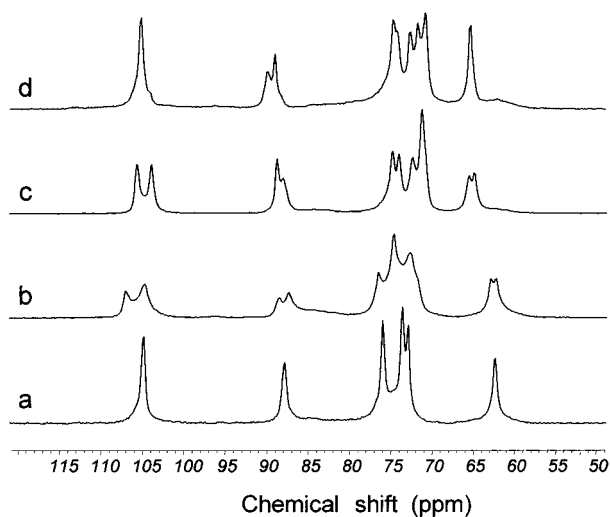


**Figure 3.**  $^{13}\text{C}$  CP/MAS NMR spectra of (a) cellulose III<sub>I</sub>, (b) microcrystalline cellulose II, (c) I<sub>β</sub> cellulose from tunicate, and (d) I<sub>α</sub> cellulose from *Glaucocystis*.

the C4 of cellulose III<sub>I</sub> is exactly in the middle of the doublet of the C4 of cellulose II. Thus, the spectrum of cellulose III<sub>I</sub> can be considered as being very close from a subset of the spectrum of cellulose II.

**FT-IR Spectra.** A typical spectrum of cellulose III<sub>I</sub> recorded with nonpolarized radiation is shown in Figure 4a, where the spectrum in part a corresponds to the region 3600–2800  $\text{cm}^{-1}$  and the spectrum in part b to the region 1500–500  $\text{cm}^{-1}$ . Both diagrams display very sharp absorption peaks denoting the high crystallinity of the sample. In the OH stretching region, a very sharp and unusual absorption peak is observed at 3481  $\text{cm}^{-1}$  together with two broader peaks near 3270 and 3134  $\text{cm}^{-1}$ . The polarized FT-IR spectra of cellulose III<sub>I</sub> are shown in Figure 4b, where the dotted and continuous lines correspond respectively to the parallel and perpendicular situations. These spectra allow one to iden-

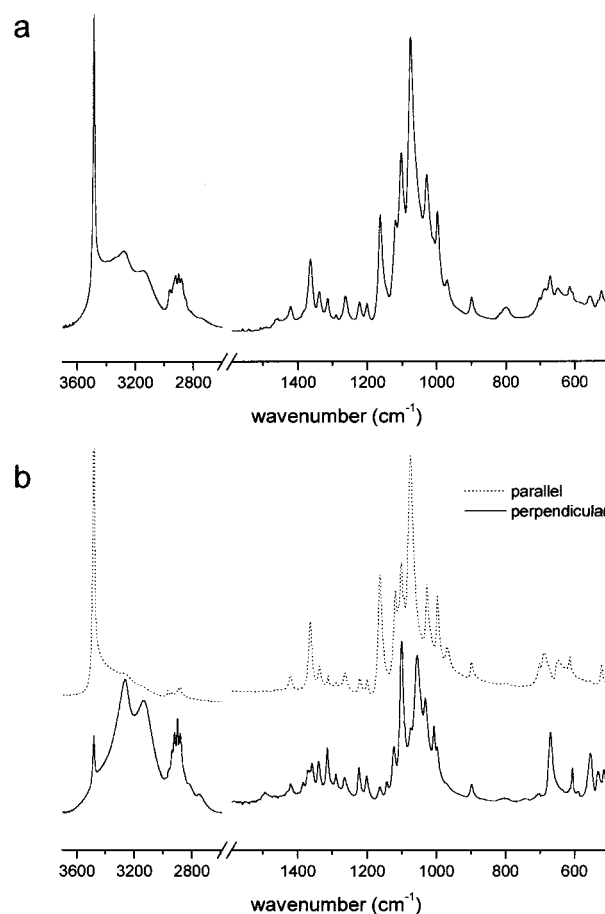


**Figure 4.** FT-IR spectra recorded on oriented films of cellulose III<sub>I</sub> films with (a) nonpolarized and (b) polarized radiation.

tify clearly the strong 3481  $\text{cm}^{-1}$  band as being parallel, whereas those at 3270 and 3134  $\text{cm}^{-1}$  correspond to a perpendicular polarization.



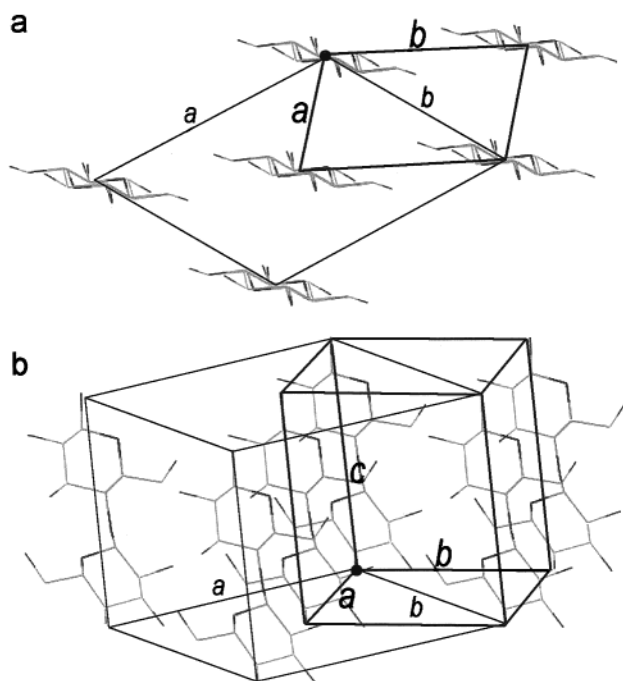


**Figure 5.** Schematic drawing of the new unit cell of cellulose III<sub>I</sub> and its orientation with respect to the unit cell of Sarko et al.:<sup>27</sup> (a) projection perpendicular to the chain axis and (b) three-dimensional representation.

## Discussion

The experimental data presented in this study bring some new insights into the nature and structure of cellulose III<sub>I</sub>. Our results are based on the solid-state conversion of highly crystalline cellulose I samples into cellulose III<sub>I</sub> using supercritical ammonia. As reported earlier,<sup>28,29</sup> this protocol yields cellulose III<sub>I</sub> samples where the orientation and the crystallinity of the parent sample are essentially maintained. The diagram resulting from our X-ray and synchrotron experiments are far better than any fiber diagrams recorded so far for cellulose III<sub>I</sub>. Besides the wealth of new diffraction intensity data, the salient result deduced from these diagrams is the definition of a new unit cell for cellulose III<sub>I</sub>. The volume of the new cell is half that of the two-chain cell reported by Sarko and his group.<sup>27</sup> This new cell contains therefore only one cellulose chain. In addition, since the probable space group for cellulose III<sub>I</sub> is  $P2_1$ , this unique chain is located on one of the 2-fold screw axis of the cell. Thus, in the cellulose III<sub>I</sub> crystal, the asymmetric residue is reduced to one glucosyl unit. A schematic drawing of our new unit cell together with its orientation within the Sarko's cell is presented in Figure 5. The one-chain situation, together with the monoclinic space group, requires a registration of the cellulose molecules within the crystal of cellulose III<sub>I</sub>. This registration which was already noticed by Sarko and co-workers in their study<sup>27</sup> indicates that cellulose III<sub>I</sub> differs from celluloses I or II where the adjacent chains are staggered by a quarter unit cell. Such a difference is responsible for the strong intensity of the 002 reflection observed in cellulose III<sub>I</sub> as opposed to a weak 002 in celluloses I and II.

The modification from the staggered chains situation in cellulose I to the registration of these chains in cellulose III<sub>I</sub> must take place during the intermediate complex formation, when ammonia enters the crystalline lattice of cellulose I to give the well-known crystal-

line cellulose/ammonia complex.<sup>36</sup> So far, this complex has not been described in full detail, but reliable molecular details are known on the parent crystalline cellulose/diamine complexes which also lead to cellulose III<sub>I</sub> after the diamine is washed off. These complexes have been studied by X-ray diffraction analysis<sup>37,38</sup> and <sup>13</sup>C CP/MAS NMR spectroscopy.<sup>39,40</sup> These techniques have revealed that in these complexes the hydroxymethyl moieties of cellulose were rotated from *tg* to *gt* under the influence of diamine complexant. As mentioned by Blackwell et al.,<sup>38</sup> the effect of these complexants was to break the intermolecular hydrogen bonds that held the cellulose structure together. Concomitant with this action, the complexant induced a shifting of the cellulose chains which rearranged themselves from a quarter stagger to a register stacking. Despite a lack of detailed structural study on the cellulose/ammonia complex, we believe that the same mechanism of hydrogen bond breaking followed by chain shifting must occur when ammonia penetrates into the cellulose lattice to yield the cellulose/ammonia crystalline complex.

The definition of a one-chain unit cell for cellulose III<sub>I</sub> is not new in the field of cellulose. Indeed, besides cellulose I<sub>α</sub> which is a one-chain triclinic cell, two one-chain monoclinic cells have also been described for cellulose diamine complexes, namely, the cellulose/1,3 diaminopropane and cellulose/1,2 diaminopropane.<sup>38</sup> In both complexes as well as in the present cellulose III<sub>I</sub>, the unit cells together with the  $P2_1$  space group prescribe a registration of the chains within the crystalline lattice.

The electron microscopy and electron diffraction data presented in Figure 2 corroborate earlier experiments where *Valonia* microfibrils were converted into cellulose III<sub>I</sub> after repeated swelling in ethylenediamine and washing in dry methanol.<sup>41–43</sup> During such treatment, achieved at room temperature, each cellulose I microfibril was essentially converted into cellulose III<sub>I</sub> without apparent loss of external morphology. Nevertheless, high-resolution lattice images<sup>42</sup> as well as diffraction contrast images on microfibrils cross sections<sup>43</sup> revealed that within each microfibril the crystalline domains became smaller as a result of the transformation. In the present case, such thorough analysis has not been achieved, but the superior quality of the electron diffraction pattern shown in Figure 2 suggests that the present samples have larger crystalline domains than those resulting from ethylenediamine treatments at room temperature. The electron diffraction patterns such as the one shown in Figure 2 were obtained at low temperature. These patterns recorded on one crystal are fully consistent with the monoclinic symmetry deduced from the X-ray and synchrotron fiber diffraction diagrams. It is interesting to note that the electron diffraction patterns do not show the extra meridional spots 003 nor any odd order 00 $l$ . Thus, the probable  $P2_1$  space group appears to be confirmed.

Despite their high perfection, the crystals of cellulose III<sub>I</sub> obtained in this study, as well as in previous reports, correspond nevertheless to a metastable state for cellulose. Indeed, upon hydrothermal annealing, the cellulose III<sub>I</sub> crystals normally revert completely to the more stable cellulose I.<sup>41</sup> Less expected was the present observation, which indicates that a limited reversion could also occur in the dry state under an electron beam

irradiation at room temperature. Such phenomenon, which does not take place at liquid-nitrogen temperature, must be due to the swelling of the cellulose lattice during irradiation with an electron beam. Such swelling, which has already been reported for *Valonia* cellulose at room temperature,<sup>44</sup> is less severe at low temperature since the radiation damage of cellulose, and therefore its swelling, is significantly reduced when the sample temperature is lowered by a liquid-nitrogen environment.

The <sup>13</sup>C CP/MAS spectrum of cellulose III<sub>I</sub>, shown in Figure 3, is of better resolution than the spectra reported so far for this cellulose allomorph.<sup>16,26</sup> The occurrence of only one signal per carbon atom confirms that in this allomorph, it is the glucosyl residue that is the magnetically independent entity, in full agreement with the results from our diffraction data which showed that this glucosyl residue was also the crystallographic asymmetric unit. Following the observations of Horii et al.,<sup>17</sup> the occurrence of a chemical shift for C6 at 62.3 ppm confirms that the hydroxymethyl group of the glucosyl residue is in the *gt* conformation. Thus the C6 conformation of cellulose III<sub>I</sub> differs from that of the parent cellulose I for which the hydroxymethyl groups are believed to be in the *tg* conformation.

As aforementioned, the comparison of the chemical shifts of C1, C4, and C6 of cellulose III<sub>I</sub> with those of the other cellulose allomorphs indicates some similarity between the spectra of celluloses III<sub>I</sub> and II. In the spectrum of cellulose II, the signals of C1, C4, and C6 carbons occur as doublets,<sup>45</sup> indicating that there are two magnetically nonequivalent glucosyl residues per unit cell. From the recent crystallography data on celldextrins<sup>18–20</sup> and cellulose II,<sup>21–23</sup> we know that in this allomorph, there are two cellulose chains per unit cell and that in each chain the glucosyl moieties are connected by a 2<sub>1</sub>-screw symmetry. Furthermore, the two chains of this allomorph have substantial conformational differences: in one of the chains, namely, the center chain, the rings of the glucosyl moieties are more puckered than in the other. In addition, there is also a difference of 10° for the *τ* torsion angle of the glycosidic linkage between one of the chain and the other. We believe that these differences are responsible for the dual resonance of the C1, C4, and C6 of cellulose II. In light of the nearly perfect match of the chemical shift of C1 and C6 of cellulose III<sub>I</sub> and the upfield peak of the corresponding doublets of cellulose II, we may speculate that the conformation of the single chain of cellulose III<sub>I</sub> bears substantial similarities with one of the two nonequivalent chains of cellulose II. Thus, if a new crystal structure of cellulose III<sub>I</sub> could be refined, one could tentatively assign each peak in the resonance doublets of C1, C4, and C6 to the origin or center chain of cellulose II.

The infrared spectra shown in Figures 4 show with better resolution the same features as the cellulose III<sub>I</sub> spectra reported already in the literature.<sup>46</sup> In our spectra, the OH stretching region is remarkable. Indeed, unlike for the other allomorphs of cellulose, which show broader OH stretching band, this region is dominated by the very strong and narrow parallel (||) absorption band at 3481 cm<sup>-1</sup>. At this rather high wavenumber, this band corresponds to a somewhat weak hydrogen bond.<sup>47</sup> On the other hand, its sharpness is an indication that the geometry of this hydrogen bond is quite well defined. Following the arguments of Kondo,<sup>48</sup> such a

narrow band should be attributed to an intramolecular hydrogen bond which is not perturbed by any mixing with intermolecular hydrogen bond. Since the conformation of the hydroxymethyl group in cellulose III<sub>I</sub> appears to be *gt*, it is likely that the parallel (||) band near 3481 cm<sup>-1</sup> corresponds to the classical O3...O5'<sup>49</sup> hydrogen bond which occurs in all crystalline celluloses. Another possibility would be O3...O6', but in the *gt* conformation, this bond would be substantially larger than 0.3 nm and therefore at the limit of the hydrogen bonding.

As in the case of <sup>13</sup>C CP/MAS NMR, it is interesting to compare the OH stretching region of our cellulose III<sub>I</sub> samples with those of the other cellulose allomorphs. Remarkably, it is again cellulose II that shows sharp and narrow absorption bands in this region, with two parallel bands at 3447 and 3488 cm<sup>-1</sup>.<sup>50</sup> These bands have been attributed to intramolecular hydrogen bonds, likely the O3...O5'.<sup>50</sup> In the center chain of cellulose II, the distance between O3 and O5 cellulose is 0.266 and 0.273 nm for the origin chain.<sup>23</sup> Thus, in cellulose II, the band near 3447 cm<sup>-1</sup> can be tentatively attributed to the O3...O5' hydrogen bond of the center chain and the band at 3488 cm<sup>-1</sup> to the origin chain. Following this reasoning, one can speculate that the parallel band at 3481 cm<sup>-1</sup> in the present cellulose III<sub>I</sub> samples can be attributed to an intramolecular O3...O5' hydrogen bond with a distance between the two oxygen atoms on the order of 0.27 nm. By extrapolating to the chain conformation, this would imply that the cellulose chain of cellulose III<sub>I</sub> would bear some resemblance with the origin chain of cellulose II.

In the spectra recorded in Figures 4b, the two broader bands near 3270 and 3134 cm<sup>-1</sup> are perpendicular. They must correspond to some intermolecular hydrogen bonds, likely between the C6 of one chain and the C2 of the next one. Their assignment appears less straightforward than in the case of the parallel band at 3481 cm<sup>-1</sup>.

When adding the crystallographic and spectroscopic data presented in this paper, the crystal of cellulose III<sub>I</sub> appears much less complex than its earlier description.<sup>27</sup> Indeed our data indicate that its crystal structure should be totally defined by determining the coordinates of 6 carbon, 5 oxygen and 10 hydrogen atoms. We have presently collected synchrotron and neutron fiber diffraction data to 0.1 nm resolution that in principle should allow this determination when the diagrams will be deconvoluted. Even if a new refinement of the structure of cellulose III<sub>I</sub> is not on the top of the priority list of the cellulose allomorphs, its structure determination and its simplicity will have important implications for understanding the crystallography and spectroscopy of other cellulose allomorphs. We have speculated on the similarity of the conformation of the cellulose chain in cellulose III<sub>I</sub> and that of the origin chain in cellulose II. It remains to be seen whether this hypothesis can be confirmed by a structure determination. Work is in progress to verify this point.

**Acknowledgment.** The authors thank Drs. B. Ras-mussen and M. Müller from ESRF for their help with the data collection at the beamline ID2. Y.N. thanks the French Government and the Japanese Society for the Promotion of Science for financial support. Part of this work was also supported by a JSPS/CNRS joint research project.

## References and Notes

- (1) Atalla, R. H.; VanderHart, D. L. *Science* **1984**, 222, 283.
- (2) VanderHart, D. L.; Atalla, R. H. *Macromolecules* **1984**, 17, 1465.
- (3) Larsson, P. T.; Wickholm, K.; Iversen, T. *Carbohydr. Res.* **1997**, 202, 19.
- (4) Horii, F.; Hirai, A.; Kitamaru, R. *Macromolecules* **1987**, 20, 2117.
- (5) Newman, R. H. *Holzforschung* **1999**, 53, 335.
- (6) Gardner, K. H.; Blackwell, J. *Biopolymers* **1974**, 13, 1975.
- (7) Sarko, A.; Muggli, R. *Macromolecules* **1974**, 7, 486.
- (8) Sugiyama, J.; Vuong, R.; Chanzy, H. *Macromolecules* **1991**, 24, 4168.
- (9) Heiner, A. P.; Sugiyama, J.; Teleman, O. *Carbohydr. Res.* **1995**, 273, 207.
- (10) Kroon-Batenburg, L. M. J.; Kroon, J. *Glycoconjugate J.* **1997**, 14, 677.
- (11) Aabloo, A.; French, A. D. *Macromol. Theory Simul.* **1994**, 3, 185.
- (12) Stipanovic, A. J.; Sarko, A. *Macromolecules* **1976**, 9, 851.
- (13) Kolpak, F. J.; Blackwell, J. *Macromolecules* **1976**, 9, 273.
- (14) The conformation of the hydroxymethyl group is defined by two letters, the first referring to the torsion angle  $\chi$  (O5–C5–C6–O6) and the second to the torsion angle  $\chi'$  (C4–C5–C6–O6). Thus, the ideal *tg* and *gt* conformations would respectively be defined as sets of two angles (180°, 60°) and (60°, 180°).
- (15) Dudley, R. L.; Fyfe, C. A.; Stephenson, P. J.; Deslandes, Y.; Hamer, G. K.; Marchessault, R. H. *J. Am. Chem. Soc.* **1983**, 105, 2469.
- (16) Isogai, A.; Usuda, M.; Kato, T.; Uryu, T.; Atalla, R. H. *Macromolecules* **1989**, 22, 3168.
- (17) Horii, F.; Hirai, A.; Kitamaru, R.; Sakurada, I. *Polym. Bulletin* **1983**, 10, 357.
- (18) Gessler, K.; Krauss, N.; Steiner, T.; Betzel, C.; Sandmann, C.; Saenger, W. *Science* **1994**, 266, 1027.
- (19) Raymond, S.; Heyraud, A.; Tran Qui, D.; Kvick, Å.; Chanzy, H. *Macromolecules* **1995**, 28, 2096.
- (20) Raymond, S.; Henrissat, B.; Tran Qui, D.; Kvick, Å.; Chanzy, H. *Carbohydr. Res.* **1995**, 277, 209.
- (21) Raymond, S.; Kvick, Å.; Chanzy, H. *Macromolecules* **1995**, 28, 8422.
- (22) Gessler, K.; Krauss, N.; Steiner, T.; Betzel, C.; Sarko, A.; Saenger, W. *J. Am. Chem. Soc.* **1995**, 117, 11397.
- (23) Langan, P.; Nishiyama, Y.; Chanzy, H. *J. Am. Chem. Soc.* **1999**, 121, 9940.
- (24) Hess, K.; Trogus, C. *Ber. Dtsch. Chem. Ges.* **1935**, 68B, 1986.
- (25) Davis, W. E.; Barry, A. J.; Peterson, F. C.; King, A. J. *J. Am. Chem. Soc.* **1936**, 65, 1294.
- (26) Chanzy, H.; Henrissat, B.; Vincendon, M.; Tanner, S. F.; Belton, P. S. *Carbohydr. Res.* **1987**, 160, 1.
- (27) Sarko, A.; Southwick, J.; Hayashi, J. *Macromolecules* **1976**, 9, 857.
- (28) Yatsu, L. Y.; Calamari, T. A.; Benerito, R. R. *Text. Res. J.* **1986**, 56, 419.
- (29) Isogai, A.; Usuda, M. *Mokuzai Gakkaishi* **1992**, 38, 562.
- (30) Nishiyama, Y.; Kuga, S.; Wada, M.; Okano, T. *Macromolecules* **1997**, 30, 6395.
- (31) Belton, P. S.; Tanner, S. F.; Cartier, N.; Chanzy, H. *Macromolecules* **1989**, 22, 1615.
- (32) Imai, T.; Sugiyama, J.; Itoh, T.; Horii, F. *J. Struct. Biol.* **1999**, 127, 248.
- (33) Battista, O. A. In *Microcrystal Polymer Science*; McGraw-Hill Book Co: New York, 1975; pp 17–57.
- (34) Wade, R. H.; Creely, J. J. *Text. Res. J.* **1974**, 41, 941.
- (35) Imai, T.; Sugiyama, J. *Macromolecules* **1998**, 31, 6275.
- (36) Barry, A. J.; Peterson, F. C.; King, A. J. *J. Am. Chem. Soc.* **1936**, 58, 333.
- (37) Lee, D. M.; Burnfield, K. E.; Blackwell, J. *Biopolymers* **1984**, 23, 111.
- (38) Blackwell, J.; Kurz, D.; Su, M.-Y.; Lee, D. L. In *The Structure of Cellulose: Characterization of the Solid State*; Atalla, R. H., Ed.; ACS Symposium Series 340; American Chemical Society: Washington, D.C., 1987; pp 199–213.
- (39) Henrissat, B.; Marchessault, R. H.; Taylor, M. G.; Chanzy, H. *Polym. Commun.* **1987**, 28, 113.
- (40) Kunze, J.; Fink, H.-P. *Das Papier* **1999**, 53, 753.
- (41) Roche, E.; Chanzy, H. *Int. J. Biol. Macromol.* **1981**, 3, 201.
- (42) Sugiyama, J.; Harada, H.; Saiki, H. *Int. J. Biol. Macromol.* **1987**, 9, 122.
- (43) Chanzy, H.; Henrissat, B.; Vuong, R.; Revol, J. F. *Holzforschung* **1986**, 40, (Suppl. 45).
- (44) Revol, J. F. *J. Mater. Sci. Lett.* **1985**, 4, 1347.
- (45) In the <sup>13</sup>C CP/MAS spectrum of cellulose II presented here, a significant splitting is seen at C6 (62.9 and 62.2 ppm). We believe that it is the first time that such splitting has been observed.
- (46) Mann, J.; Marrinan, H. J. *J. Polym. Sci.* **1958**, 32, 357.
- (47) Novak, A. *Struct. Bonding* **1974**, 18, 177.
- (48) Kondo, T. In *Polysaccharides: Structural Diversity and Functional Versatility*; Dumitriu, S., Ed.; Marcel Dekker: New York, 1998; pp 131–172.
- (49) Primed atoms are in adjacent residues of the same cellulose chain.
- (50) Marchessault, R. H.; Liang, C. Y. *J. Polym. Sci.* **1960**, 43, 71.

MA001406Z